Spectrum Compression Space–Time Adaptive Processing for TOPS SAR System

Xueshi Li, Mengdao Xing, *Member, IEEE*, Yimin D. Zhang, *Senior Member, IEEE*,
Guang-Cai Sun, *Member, IEEE*, Yi Liang, and Zheng Bao, *Life Senior Member, IEEE*

Abstract—A multichannel terrain observation by progressive scans (TOPS) synthetic aperture radar (SAR) system is capable of imaging a wider swath with a higher azimuth resolution for improved moving target detection. For TOPS SAR, due to antenna beam steering, the azimuth bandwidth of background clutter is much larger than the instantaneous signal bandwidth. To overcome this problem, a method referred to as spectrum compression space–time adaptive processing (SC-STAP) is proposed in this letter. Through the SC process, both the Doppler spectrum and the spatial spectrum of the background clutter are simultaneously compressed. This key step achieves fully overlapped clutter space–time spectrum lines and, as such, enables effective clutter suppression and target signal alias compensation by applying linearly constrained STAP. Furthermore, in order to avoid the target ambiguities arising from the spectral wrapping, an approach based on deramp processing is proposed to focus the moving targets for TOPS SAR mode. Simulation results validate the effectiveness of the proposed algorithm.

Index Terms—Moving target, multichannel, space–time adaptive processing (STAP), spectrum compression (SC), terrain observation by progressive scans (TOPS) synthetic aperture radar (SAR).

I. Introduction

EQUIPPING terrain observation by progressive scans (TOPS) synthetic aperture radar (SAR) with a multichannel capability enables imaging of an ultrawide swath with a long observation time [1]. As such, the multichannel TOPS SAR system becomes an attractive choice for moving-target detection and imaging. In addition, exploiting a long observation time can enhance the signal-to-noise ratio of moving targets. Space–time adaptive processing (STAP) is a powerful technique for clutter suppression in a multichannel stripmap SAR system [2]. Existing STAP techniques, however, are not suitable for multichannel TOPS SAR systems because the resulting azimuth bandwidth of background clutter in these systems is much larger than the instantaneous signal bandwidth.

In this letter, we propose a spectrum compression (SC)-STAP method to achieve effective clutter suppression, which fundamentally stems from the deramping approach used in the SAR focusing of TOPS [3]–[5] or spotlight [6] data. However, unlike these approaches, which solve the linear variation of the Doppler centroid only along the azimuth dimension so as to avoid the azimuth aliasing in the Doppler domain, the proposed SC processing is applied to compress both the Doppler spectrum and the spatial spectrum of the background clutter in the joint space–time domain and, as such, enables effective STAP for TOPS SAR systems. Through this processing, the space–time spectrum lines of the background clutter become fully overlapped, whereas the moving target exhibits a Doppler shift that is separated from the background clutter, facilitating the placement of a deep notch on the clutter ridge for efficient clutter suppression.

On the other hand, for multichannel TOPS SAR systems, the pulse repetition frequency (PRF) is often designed to be smaller than the instantaneous clutter bandwidth. In this case, the target signal is aliased and may cause ghost targets in the resulting azimuth Doppler-range map. To overcome this problem, linear constraints can be introduced in the space–time plane for effective ghost target suppression. This procedure is similar to the linearly constrained minimum variance technique in array signal processing [7]. Furthermore, Doppler spectrum wrapping, which arises from the cross-track (c.t.) velocity of the moving target, creates target ambiguities. This problem is resolved in the proposed method by postprocessing the results using the deramp approach.

This letter is organized as follows. The signal model of moving targets for a multichannel TOPS SAR is introduced in Section II. In Section III, the proposed full-aperture TOPS SAR ground moving-target indication (GMTI) processing scheme is described. The SC-STAP method, which consists of the SC and the linearly constrained STAP processes, is then proposed. A moving-target focusing algorithm based on deramp processing is then followed. Simulation results are provided in Section IV to validate the proposed method. Finally, Section V concludes this letter.

II. Singnal Model of Moving Targets for Multichannel TOPS SAR

The geometry of an M-channel TOPS SAR is shown in Fig. 1. The SAR platform moves along the X-axis with velocity of v. The reference channel transmits a signal, and the echoed waveforms are received at all M channels. The offset from channel m to the reference channel is denoted as X_m, where $m = 1, 2, \ldots, M$. The instantaneous slant range between the moving target P and channel m can be obtained as

$$R_m(t_a) = \sqrt{(R_b + v_r t_a)^2 + (vt_a + X_m - v_a t_a - vt_c)^2}$$

$$\approx R_b + v_r t_a + ((v - v_a)t_a - vt_c + X_m)^2 / (2R_b) \quad (1)$$

Fig. 1. Distance history of a moving target for multichannel TOPS SAR.

where t_a is the azimuth slow time, t_c is the Doppler centroid time, vt_c and R_b are the azimuth position and the nearest slant range of the target, and v_r and v_a denote the c.t. and along-track (a.t.) velocities of the moving target, respectively.

Assume that a linear frequency modulation waveform is transmitted from the reference channel. Then, the signal returned from a moving target P and received at channel m can be expressed as

$$s(t_r, t_a; X_m) = w_r(t_r)w_{az}(t_a - t_s + X_m/2v)w_{an}(X_m)$$
$$\times \exp\left(j\pi\gamma\left(t_r - (R_c(t_a) + R_m(t_a))/c\right)^2\right)$$
$$\times \exp(-j2\pi(R_c(t_a) + R_m(t_a))/\lambda) \quad (2)$$

where t_r is the fast time, $R_c(t_a)$ is the instantaneous slant range of the reference channel, t_s is the center illuminated time of the moving target P, c is the propagation velocity of light, γ is the chirp rate of the transmitted signal, and λ is the wavelength. In addition, $w_r(\cdot)$ denotes the range window function, $w_{az}(\cdot)$ denotes the azimuth window function, and $w_{an}(\cdot)$ is the weight function of channels.

After range compression and compensating the constant exponent term, the received signal becomes

$$s(t_r, t_a; X_m) = w_r\left(t_r - 2R_{\frac{m}{2}}(t_a)/c\right)w_{az}(t_a - t_s + X_m/2v)$$
$$\times w_{an}(X_m)\exp\left(-j4\pi R_{\frac{m}{2}}(t_a)/\lambda\right) \quad (3)$$

where $R_{m/2}(t_a) = \sqrt{(R_b + v_r t_a)^2 + (vt_a + X_m/2 - v_a t_a - vt_c)^2} \approx R_b + v_r t_a + (vt_a + X_m/2 - v_a t_a - vt_c)^2/2R_b$.

III. CLUTTER SUPPRESSION AND MOVING-TARGET FOCUSING METHODS

Detection and imaging of moving targets require the background clutter to be effectively suppressed. Here, we propose the SC-STAP method to achieve effective clutter suppression and then introduce a moving-target focusing method that incorporates the deramp processing.

A. Description of the Full-Aperture TOPS SAR-GMTI Processing Scheme

Fig. 2 shows the proposed full-aperture TOPS SAR-GMTI processing scheme. First, the SC process is carried out on the range-compressed data. As a result of this step, both the Doppler spectrum and the spatial spectrum of the background clutter are simultaneously compressed, and their space–time spectrum lines become fully overlapping. Clutter suppression is then performed by utilizing the linearly constrained STAP
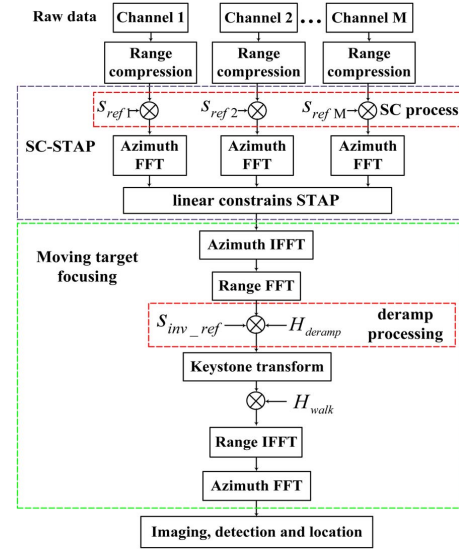
Fig. 2. Full-aperture TOPS SAR-GMTI processing scheme.

based on the obtained space–time spectrum. Finally, the deramp processing focuses the moving target in the azimuth frequency domain.

B. Analysis of Space–Time Plane After SC Process

Equation (3) is transformed into the joint Doppler–angle domain, expressed as (the range window function is temporarily ignored)

$$S(f_a, \sin\theta) = W_{az}\left(\frac{vt_c}{(v-v_a)} - \frac{R_b(f_a\lambda/2 + v_r)}{(v-v_a)^2} - t_s\right)$$
$$\times W_{an}\left(\frac{1}{\lambda}\left(\sin\theta - \frac{(\lambda f_a + 2v_r)}{2(v-v_a)}\right)\right)$$
$$\times \exp\left(-j\frac{4\pi}{\lambda}R_b\right)$$
$$\times \exp\left(j\frac{\pi\lambda R_b}{2(v-v_a)^2}\left(f_a + \frac{2}{\lambda}v_r\right)^2\right)$$
$$\times \exp\left(-j\frac{2\pi vt_c}{(v-v_a)}\left(f_a + \frac{2}{\lambda}v_r\right)\right) \quad (4)$$

where θ is the azimuth angle, and $W_{an}(\cdot)$ is the Fourier transform (FT) of $w_{an}(\cdot)$, which is a sinc function. It can be observed from (4) that angle θ and Doppler frequency f_a of the moving targets satisfy the following relationship in the space–time plane: $f_a = 2(v - v_a)\sin\theta/\lambda - 2v_r/\lambda$. Specifically, by setting the velocity of the moving target to zero, we can obtain the relationship between the angle and the Doppler frequency of the background clutter, expressed as $f_a = 2v\sin\theta/\lambda$. In order to clearly describe the difference between the stripmap SAR and the TOPS SAR, we depict their space–time spectrum lines in Fig. 3(a) and (b), respectively. In Fig. 3(a), the solid line C represents the overlapping background clutter, and the dashed line T represents the moving target. In Fig. 3(b), the solid lines C_1, C_2, and C_3, respectively, represent the signals from three stationary targets with distinct azimuth angles, and the dashed lines T_1, T_2, and T_3 represent those of the moving targets. In TOPS SAR mode, the antenna is rotated throughout the acquisition from backward to forward. Therefore, targets
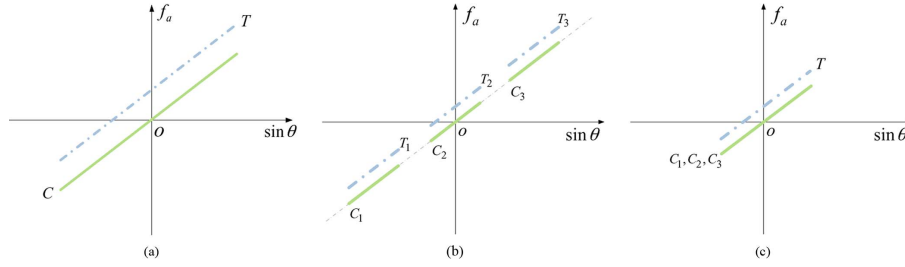
Fig. 3.   Space–time spectrum lines. (a) Stripmap SAR mode. (b) TOPS SAR mode. (c) TOPS SAR mode after SC process.

in different azimuth positions experience different Doppler histories, which lead to the clutter spectrum lines that do not fully overlap. Since the a.t. velocity of the moving targets is much smaller than that of the SAR platform, particularly in a spaceborne SAR system, we assume that the Doppler shift of the moving targets relative to background clutter is only due to the c.t. velocity.

The clutter alias problem can be mitigated by reducing the clutter Doppler spectrum and the corresponding supporting area of angle, as illustrated in Fig. 3(c). In Fig. 3(c), the solid line represents the completely overlapping Doppler signature of the clutter, and the dot-dash line represents that of the moving target. Such clutter SC is achieved by multiplying the signal, expressed in (3), by the following SC reference function:

$$s_{\text{ref}}(t_a, X_m) = \exp\left(-j\pi k_{\text{rot}}(t_a + X_m/2v)^2\right) \tag{5}$$

where $k_{\text{rot}} = 2v^2/\lambda R_{\text{ref}}$ denotes the slope, and R_{ref} denotes the rotation range distance [3]–[5]. The SC process simultaneously compresses both the Doppler spectrum and the spatial spectrum of the background clutter so as to obtain fully overlapping clutter space–time spectrum lines, which can then be effectively suppressed using STAP. It is noted that the spectrum of the clutter as well as the targets is stretched after (5) is applied. This fact is considered in the following clutter suppression and moving-target focusing process. After performing the 2-D FT of the product of (3) and (5), we obtain

$$
\begin{aligned}
&S(f_a, \sin\theta) \\
&= \int w_{az}(t - t_s) \\
&\quad \times \exp\left(-j4\pi\left(R_b + v_r t + (vt - v_a t - vt_c)^2/2R_b\right)/\lambda\right) \\
&\quad \times \exp(-j\pi 2v^2 t^2/\lambda R_{\text{ref}}) \exp(-j2\pi f_a t)\Omega(t)dt \tag{6}
\end{aligned}
$$

where $\Omega(t) \approx W_{an}((\sin\theta/\lambda) - (f_a/2v) - (v_r/\lambda v) - (v_a\sin\theta/\lambda v))$, $t = t_a + (x/2v)$, $x = X_m$, and $W_{an}(\cdot)$ is a sinc function. It is clear that, in the sinc function ridges, the Doppler frequency and the angle of the moving target are related by $f_a = 2(v - v_a)\sin\theta/\lambda - 2v_r/\lambda$, which defines the space–time spectrum lines of the background clutter when the velocity of the moving target is set to zero. After the SC process, the supporting areas of clutter overlap in the space–time plane [see Fig. 3(c)].

C. SC-STAP Method for Clutter Suppression

Now, we perform clutter suppression based on the post-SC data. Considering the case that the PRF is smaller than the instantaneous signal bandwidth, aliasing will occur in each

channel. In this case, by transforming (6) into the array domain, we obtain

$$
\begin{aligned}
S(f_a, X_m) = &\sum_{i=1}^{N} w_{an}(X_m) \\
&\times \exp\left(j2\pi X_m(f_a + i \cdot \text{PRF} + 2v_r/\lambda)/2v\right) \\
&\times \exp\left(j\Phi_1\right) \int w_{az}(t - t_s)\exp(j\Phi_2) \\
&\times \exp\left(-j\pi 2v^2 t^2/\lambda R_{\text{ref}} - j2\pi(f_a + i \cdot \text{PRF})t\right) \\
&\times \exp\left(-j4\pi\left(R_b + v_r t \right.\right. \\
&\quad\left.\left. + (vt - vt_c - v_a t)^2/2R_b\right)/\lambda\right)dt \tag{7}
\end{aligned}
$$

where $\Phi_1 = -2\pi v_a^2(X_m/2v)^2/\lambda R_b$, and $\Phi_2 = -2\pi v_a(t - t_c - v_a t/v)X_m/\lambda R_b$. As the result of the aliased signal representations of moving targets, ghost targets may appear unless the ambiguity due to target aliasing is properly avoided. The effect of ghost targets to the moving-target detection is more pronounced if the target signal-to-clutter-plus-noise ratio (SCNR) after clutter suppression is high. To effectively suppress the ghost target problem due to aliasing, we introduce linear constraints [7] to the STAP. Compared with the multichannel reconstruction proposed in [1], which provides the optimum solution for the suppression of the azimuth ambiguities of a band-limited signal, the proposed STAP with the linear constraints minimizes the power of both ambiguous signal components and the undesired clutter and jamming [2]. Utilizing the linear constraints, depicted in (8b), that the expected signal component of the moving target is set to unity and the aliased signal components are set to zero, the weight vector that achieves clutter suppression can be obtained from [2] as

$$\min_{\mathbf{w}_i} \quad \mathbf{w}_i^H \mathbf{R_s} \mathbf{w}_i \tag{8a}$$

$$\text{s.t.} \quad \mathbf{w}_i^H \mathbf{C}_i = \mathbf{f} \tag{8b}$$

for $i = 1, 2, \ldots, N$, where the covariance matrix $\mathbf{R_s} = E\{\mathbf{S}(f_a, \mathbf{X})\mathbf{S}^H(f_a, \mathbf{X})\}$ is estimated from the post-SC data, $\mathbf{S}(f_a, \mathbf{X}) = [S(f_a, X_1), \ldots, S(f_a, X_m)]^T$, $\mathbf{C}_i = [\mathbf{a}_i, \mathbf{a}_1, \ldots, \mathbf{a}_{i-1}, \mathbf{a}_{i+1}, \ldots, \mathbf{a}_N]$ is the constrained matrix, $\mathbf{f} = [1, 0, \ldots, 0]^T$ is the corresponding constrained vector, and $\mathbf{a}_i(f_a, \mathbf{X}) = \exp(j2\pi(f_a + i \cdot \text{PRF} + 2v_r/\lambda) \cdot \mathbf{X}/2v)$ is the steering vector of the moving target. We refer to the above clutter suppression processing, which combines both the SC and the linearly constrained STAP, as the SC-STAP method. In this method, the steering vector depends on the parameter of the c.t. velocity of the moving target. The velocity of the moving target can be estimated by maximizing the target SCNR [8], which is defined in the image domain as the ratio

between the moving-target peak signal power and the average clutter-plus-noise power.

D. Focusing Algorithm for the Moving Target

In order to avoid the moving-target ambiguities caused by the Doppler spectrum wrapping, an approach based on deramp processing [9] is proposed to focus the moving targets for TOPS SAR mode in this section. Applying the azimuth inverse FT (IFT) and range FT to (7) yields

$$
\begin{aligned}
S(f_r, t_a) = & W_r(f_r) w_{az}(t_a - t_s) \\
& \times \exp\left(-j4\pi(f_c + f_r)(R_b + v_r t_a)/c\right) \\
& \times \exp\left(-j2\pi(f_c + f_r)(vt_a - vt_c - v_a t_a)^2/cR_b\right) \\
& \times \exp\left(-j\pi 2v^2 t_a^2/\lambda R_{\mathrm{ref}}\right).
\end{aligned} \tag{9}
$$

The last term of (9) is caused by SC and needs to be compensated. Then, the moving target can be focused by performing deramp processing, which multiplies signal by the following deramp reference function:

$$
H_{\mathrm{deramp}}(f_r, t_a) = \exp\left(\frac{j2\pi(f_c + f_r)(vt_a - v_a t_a)^2}{cR_b}\right). \tag{10}
$$

It is noted that the range walk observed in (9) cannot be corrected by the Keystone transform when the phase of the complex signals is wrapped. Specifically, a fast moving target or a moving target located at the edge of the observed scene may lead to phase wrapping. The filter function $H_{\mathrm{walk}} = \exp(j4\pi(f_c + f_r)\mathrm{PRF}\lambda M_{\mathrm{amb}}\tau_a/2c)$ can be applied to correct the range walk due to the ambiguity number, where M_{amb} is an integer, referred to as the ambiguity number. This ambiguity number can be estimated, along with other parameters, by maximizing the target SCNR, as described in Section III-C. After performing the Keystone transform and filter operation, the range IFT and azimuth FT can be used to focus the moving target. The focused result is

$$
\begin{aligned}
s(t_r, f_\eta) = & w_r\left(t_r - \frac{2R_b}{c} - \frac{v^2 t_c^2}{cR_b}\right) W_{az}\left(f_\eta + \frac{2v_{\mathrm{rem}}}{\lambda}\right) \\
& \times \exp\left(-j\frac{4\pi}{\lambda}R_b\right) \exp\left(-j\frac{2\pi v^2 t_c^2}{\lambda R_b}\right)
\end{aligned} \tag{11}
$$

where f_η denotes the new azimuth frequency corresponding to τ_a, and v_{rem} denotes the baseband velocity [9]. After imaging the moving target, detection can be performed in the image domain. We note in (11) that the focused position is located in azimuth of $f_\eta = -2v_{\mathrm{rem}}/\lambda$ and range of $\hat{t} = 2R_b/c + v^2 t_c^2/cR_b$, which is not the true position. The true position can be obtained by utilizing the relationship between the baseband velocity [9] and the real c.t. velocity of the moving target.

IV. SIMULATION RESULTS

Here, simulation results are provided to validate the proposed method. The system parameters are listed in Table I. The amplitude and phase of the background clutter are assumed to follow the Rayleigh and uniform distributions, respectively. The noise is assumed to be additive complex Gaussian, and the clutter-to-noise ratio is assumed to be 60 dB. The emulated TOPS SAR

TABLE I
SYSTEM PARAMETERS

Carrier frequency	9.65GHz	Center line distance	514 km
Range bandwidth	18MHz	Rotational distance	102.8km
IBW	3KHz	TR modules along-track	4.8m
Azimuth bandwidth	11.2KHz	Pulse duration	1us
PRF	4.2KHz	Number of receive channels	12
Velocity	7285m/s	Maximum steering angle	0.497°
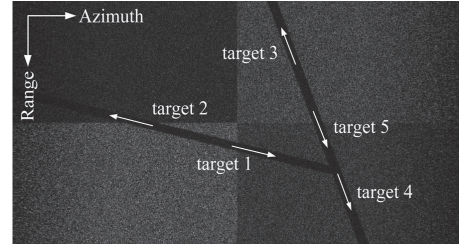
Fig. 4. Emulated background clutter image.
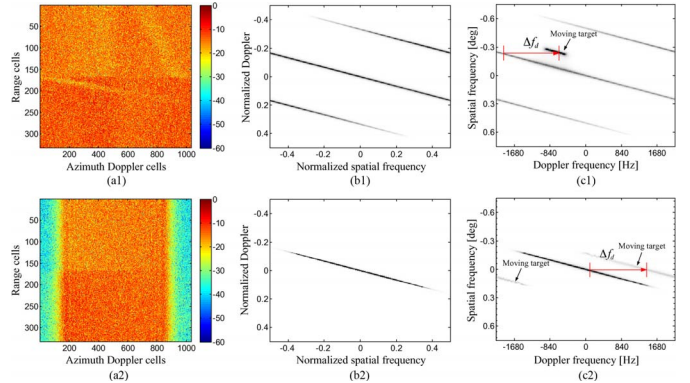
Fig. 5. Simulation results. (a1) Doppler spectrum of the background clutter without SC process and (a2) after SC. (b1) Space–time spectrum of the clutter without SC and (b2) after SC. (c1) Space–time spectrum of the clutter and the moving target without SC and (c2) after SC.

scene is focused in the slant range and azimuth Doppler plane, as seen in Fig. 4. Return signals from five targets moving along the two roads are added to the raw data set of the background clutter. The five moving targets are represented in the figure by arrows, indicating their true positions and corresponding motion directions. Their c.t. and a.t. velocities are (13.6 m/s, 23.1 m/s), (−22.4 m/s, −36.0 m/s), (−34.8 m/s, −20.4 m/s), (45.5 m/s, 10.5 m/s), and (23.7 m/s, 9.3 m/s), respectively.

Fig. 5(a1) and (a2), respectively, show the Doppler spectrum of the background clutter before and after the SC process. It is clear that, while the original Doppler spectrum of the background clutter is aliased before applying the SC, it is no longer aliased after the SC operation is performed. For the clarity of performance comparison, we start with an example where only the first target is added to the raw data set of the background clutter. Fig. 5(b1) and (b2), respectively, show the space–time spectrum of the clutter without and with the SC. In the designed TOPS SAR system, the azimuth bandwidth of clutter is 3.7 times the instantaneous signal bandwidth, and the PRF is 1.4 times the instantaneous signal bandwidth. It is clear that, while the Doppler spectrum is aliased without SC, it becomes unaliased, and the supporting angular area is
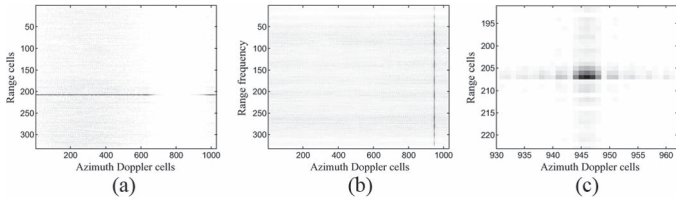
Fig. 6. Simulation results. (a) Data after clutter suppression. (b) Result after deramp processing. (c) Focusing result of the moving target.
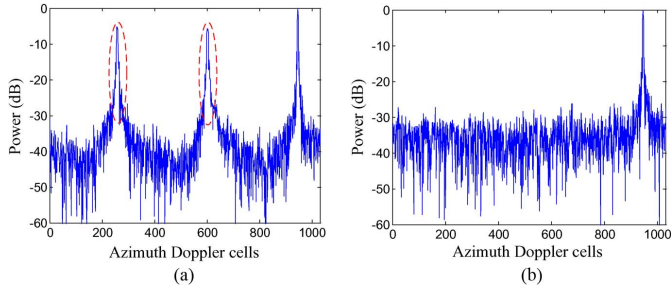
Fig. 7. Normalized power of the moving target in azimuth. (a) Without and (b) with consideration of the linear constraints.

TABLE II
MOVING-TARGET C.T. VELOCITY ESTIMATION RESULTS

Target index	Target 1	Target 2	Target 3	Target 4	Target 5
c.t. velocity (m/s)	13.6	-22.4	-34.8	45.5	23.7
Estimated values (m/s)	13.5	-22.3	-34.7	45.7	23.8
Relative error (%)	0.74	0.45	0.29	0.44	0.42

accordingly compressed after the SC operation is performed. Fig. 5(c1) and (c2), respectively, show the space–time spectra of the clutter and the moving target without and with the SC. The Doppler shift Δf_d in both figures is equal to $\Delta f_d = 2v_r/\lambda$.

Fig. 6(a) shows the data after clutter suppression by utilizing the proposed SC-STAP method. The moving-target signal can now be clearly observed. Next, we perform moving-target focusing by using the deramp processing method, and the result is shown in Fig. 6(b). It is evident in Fig. 6(b) that the azimuth spectrum of the moving target is compressed. Therefore, the moving-target ambiguities caused by the Doppler spectrum wrapping can be avoided. Fig. 6(c) shows the local enlargement of the focused result of the moving target. It is clear in Fig. 6(c) that the moving target is well focused.

We now present two additional simulations to demonstrate the effectiveness of the proposed SC-STAP and compare its performance without and with the exploitation of the linear constrains in the case of signal undersampling by reducing the PRF to one third of the previous value. The normalized azimuth power of the moving target in the image domain is investigated, as seen in Fig. 7. The ghost targets cannot be suppressed when the SC-STAP method is applied without considering the linear constraints [see the two dotted circles in Fig. 7(a)]. However, the ghost targets are no longer observed in Fig. 7(b) when the linear constraints depicted in (8b) are taken into account. Therefore, it is important to apply the linear constraints if the target SCNR after clutter suppression is high.

Now, we present the simulation results of the proposed technique when the emulated raw data includes all the five
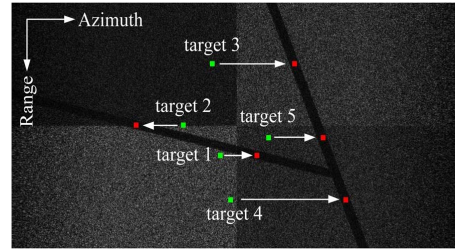
Fig. 8. Detection and location result of the moving targets. The green dots denote the detected results, whereas the red dots show the estimated target positions.

moving targets described earlier. We estimate the moving-target c.t. velocity by maximizing the target SCNR, as described in Section III-C, and the estimated results are listed in Table II. From the simulation results, it is seen that the relative error is less than 1%, which is acceptable in practice. Fig. 8 shows the final results of the detected moving targets and their locations. In Fig. 8, it is evident that all the moving targets are closely located around their respective true positions.

V. CONCLUSION

In this letter, a novel clutter suppression method, which is referred to as the SC-STAP, has been proposed for a multichannel TOPS SAR system. The SC process simultaneously compresses both the Doppler spectrum and the spatial frequency of the background clutter, and its space–time spectrum lines become fully overlapping. The ghost targets, resulted from the ambiguous signal components due to a low PRF, can be avoided by applying linear constraints in performing the STAP. In addition, the deramp processing approach is incorporated to focus the moving target in order to avoid target ambiguities caused by Doppler spectrum wrapping. Simulation results were provided to verify the effectiveness of the proposed algorithm.

REFERENCES

[1] G. Nicolas, K. Gerhard, and M. Alberto, "Multichannel azimuth processing in ScanSAR and TOPS mode operation," *IEEE Trans. Geosci. Remote Sens.*, vol. 48, no. 7, pp. 2994–3008, Jul. 2010.
[2] R. Klemm, *Principle of Space–Time Adaptive Processing*. Stevenage, U.K.: IEE, 2002.
[3] F. De Zan and A. Monti Guarnieri, "TOPSAR: Terrain observation by progressive scans," *IEEE Trans. Geosci. Remote Sens.*, vol. 44, no. 9, pp. 2352–2360, Sep. 2006.
[4] P. Prats, R. Scheiber, J. Mittermayer, A. Meta, and A. Moreira, "Processing of sliding spotlight and TOPS SAR data using baseband azimuth scaling," *IEEE Trans. Geosci. Remote Sens.*, vol. 48, no. 2, pp. 770–780, Feb. 2010.
[5] G. Sun *et al.*, "Sliding spotlight and TOPS SAR data processing without sub-aperture," *IEEE Geosci. Remote Sens. Lett.*, vol. 8, no. 6, pp. 1036–1040, Nov. 2011.
[6] R. Lanari, M. Tesauro, E. Sansosti, and G. Fornaro, "Spotlight SAR data focusing based on a two-step processing approach," *IEEE Trans. Geosci. Remote Sens.*, vol. 39, no. 9, pp. 1993–2004, Sep. 2001.
[7] B. D. Van Veen and K. M. Buckley, "Beamforming: A versatile approach to spatial filtering," *IEEE ASSP Mag.*, vol. 5, no. 2, pp. 4–24, Apr. 1988.
[8] D. Cristallini, D. Pastina, F. Colone, and P. Lombardo, "Efficient detection and imaging of moving targets in SAR images based on chirp scaling," *IEEE Trans. Geosci. Remote Sens.*, vol. 51, no. 4, pp. 2403–2416, Apr. 2013.
[9] G. Sun, M. Xing, X.-G. Xia, Y. Wu, and Z. Bao, "Robust ground moving target imaging using deramp-keystone processing," *IEEE Trans. Geosci. Remote Sens.*, vol. 51, no. 2, pp. 966–982, Feb. 2013.